# Measurement of the cascade transition via the 1st excited state of $^{16}$O in $^{12}$C$(\alpha,\gamma)^{16}$O and its S-factor in stellar helium burning

C. Matei,[1] L. Buchmann,[2,*] W.R. Hannes,[3] D. A. Hutcheon,[2] C. Ruiz,[4] C.R. Brune,[1] J. Caggiano,[2] A.A. Chen,[5] J. D'Auria,[4] A. Laird,[2,†] M. Lamey,[4,‡] ZH. Li,[2,§] WP. Liu,[6] A. Olin,[2] D. Ottewell,[2] J. Pearson,[5] G. Ruprecht,[2] M. Trinczek,[2] C. Vockenhuber,[4] and C. Wrede[4,¶]

[1]*Ohio University, Athens, OH*
[2]*TRIUMF, 4004 Wesbrook Mall, Vancouver, British Columbia, Canada, V6T 2A3*
[3]*University of Konstanz, Department of Physics, Germany*
[4]*Simon Fraser University, Burnaby, British Columbia, Canada*
[5]*McMaster University, Hamilton, Ontario, Canada*
[6]*China Institute of Atomic Energy, Beijing, P. R. China*

Radiative $\alpha$-particle capture into the first excited, J$^{\pi}$=0$^{+}$ state of $^{16}$O at 6.049 MeV excitation energy has rarely been discussed as contributing to the $^{12}$C$(\alpha,\gamma)^{16}$O reaction cross section at low energies largely due to experimental difficulties in observing this transition. We report here measurements of this radiative capture in $^{12}$C$(\alpha,\gamma)^{16}$O between and on resonances for center of mass energies of E=2.22 MeV to 5.42 MeV at the DRAGON recoil separator. To determine cross sections, the acceptance of the recoil separator including the BGO array has been simulated in GEANT as well as measured directly. The transition strength between resonances has been identified in $R$-matrix fits as resulting both from $E2$ direct capture contributions interfering with $2^+$ resonances as well as $E1$ radiative capture. Details of the extrapolation of the total cross section to low energies are then extensively discussed (S$_{6.0}$(300)=$25^{+16}_{-15}$ keV b) showing that this transition is likely the most important cascade contribution to the total cross section of $^{12}$C$(\alpha,\gamma)^{16}$O.
Last revised October 17, 2006.

PACS numbers: 24.30.Gd, 25.40.Lw, 25.40.Ny, 26.20.+f, 26.30.+k

During stellar helium burning, the two most important nuclear radiative captures are the triple-$\alpha$ and the $^{12}$C$(\alpha,\gamma)^{16}$O reactions. The relative rates of these two reactions determine the C/O abundance ratio at the end of helium burning and set the stage for the subsequent stellar evolution [1]. A reliable extrapolation of the reaction rate of $^{12}$C$(\alpha,\gamma)^{16}$O from measured to stellar helium-burning temperatures (E$\approx$300 keV) has been a longstanding problem as the cross section at this energy is too low to be measured directly ($\sigma\approx 10^{-17}$b). Yet, in stellar modeling a knowledge of that cross section to better than 10% is desirable. Part of the extrapolation problem is that the total $^{12}$C$(\alpha,\gamma)^{16}$O cross section is indeed composed of a strong ground state and several weaker cascade transitions to excited states in $^{16}$O[2]. Among the cascade transitions, some attention has been paid to the cascade transition via the 6.9 MeV[17] and 7.1 MeV excited states in $^{16}$O [3, 4], however, no consideration has been given to a possible cascade via the first excited state of $^{16}$O at 6.0 MeV and its extrapolation to low energies. This oversight is likely due to the fact that this transition is hard to observe with $\gamma$-ray detectors only, as there is no high-energy secondary $\gamma$-ray following the relatively low-energy primary $\gamma$-decay into this state. We have observed the E$\rightarrow$6.0 MeV transition in $^{12}$C$(\alpha,\gamma)^{16}$O at TRIUMF over a wide range of energies and report here the result of this observation and subsequent fits with the $R$-matrix formalism to the cross section (S-factor). We find this transition not negligible for the total cross of $^{12}$C$(\alpha,\gamma)^{16}$O at 300 keV and even more important, when higher temperature burning of $^{12}$C with helium is considered.

The experiment was carried out at the DRAGON recoil separator facility at ISAC [5]. The basic setup and data acquisition system are as described previously [5] including a BGO array around the windowless gas target for $\gamma$-ray detction and a Double-Sided-Silicon-Strip-Detector (DSSSD) for the detection of $^{16}$O recoil particles at the focal plane of DRAGON providing for $\gamma$-particle coincidences. A $^{12}$C beam of typically 30-50 pnA was delivered to the DRAGON target in the $3^+$ charge state where it encountered a windowless gas cell filled with helium with an effective length of 12.1 cm and 12.3 cm for the first and second set of runs, respectively. In the first run, the gas pressure in the cell was typically about 8 Torr, while in the second run the pressure was limited to 4 Torr, due to changed cell apertures (4 and 10 mm, respectively, see [5]), because we found the first set of pumping tubes limiting the acceptance. Therefore in the second run, the down stream pumping tubes of the gas target were enlarged to allow for an increased recoil divergence of 25 mrad. The beam size and position were monitored con-

*Electronic address: `lothar@triumf.ca`
†Present address:Department of Physics, University of York, York, UK
‡Present address:Department of Physics, University of Alberta, Edmonton,Canada
§Present address:China Institute of Atomic Energy, Beijing, P. R. China
¶Present address:Yale University, New Haven, Connecticut

tinuously by a camera in line with the gas target. The enlargement of the exit aperture of the gas target in the second set of runs resulted in a slow loss of gas out of the recirculating system into the separator. We take this pressure variation into account[6].

The beam energy was determined using the first magnet MD1 of DRAGON that has been previously calibrated [5, 7]. We used the beam of $5^+$ or $6^+$ charge state after stripping in the gas target to determine the beam energy by subsequently lowering the gas pressure and extrapolating to zero target pressure. Energies in the final analysis were, in addition, corrected for the energy loss to the center of the target. It has been found in the first set of runs that the acceptance of the DRAGON separator could be improved by tuning an energy setting of -1.0% relative to the standard [5]. We have done several measurements determining the best energy setting of DRAGON confirming this tune. The reason is that the relative stopping power difference between $^{12}$C and $^{16}$O is larger than in radiative proton capture experiments, as discussed in Refs. [5, 7].

The acceptance of the DRAGON separator drops rapidly, when the angle of the heavy reaction product exceeds ≈20 mrad[18] relative to the beam direction. This angle depends on the ratio of the net transverse momentum imparted by the decay $\gamma$ ray(s) to the momentum of the incident beam particle. Because the average net momentum for a 2-$\gamma$ decay through an intermediate state is lower than that for 1-$\gamma$ decay to the ground state, recoil acceptance can be much higher for a cascade decay than for a 1-$\gamma$ decay at the same beam energy. Observed counting rates must be corrected for acceptance and efficiency of detecting reaction products at each beam energy. Therefore the entire DRAGON system including the BGO $\gamma$-detection array has been simulated in the Monte Carlo program GEANT [8]. GEANT finds total (energy-dependent) DRAGON transmissions of 65-88% for the first set of runs and 90-95% for the second set of runs. We have performed measurements of the separator acceptance using a strong $^{148}$Gd $\alpha$ source placed at the target position. The transmission of $\alpha$ particles through the separator is 82% for a 20 mrad opening angle. To further determine the acceptance of DRAGON, we have made a measurement of the $4^+$ resonance at E=3.2 MeV in which we detected singles $\gamma$-ray, singles recoil and $\gamma$-recoil coincidence events using the large apertures. With a knowledge of the recoil charge state distribution, the acceptance of the separator can be deduced from the ratio of coincidence events to singles $\gamma$-ray events. An acceptance of 82% has been found, in accordance with the $\alpha$-source measurements. As this $4^+$ resonance decays solely by 2-$\gamma$ cascade, it is kinematically very similar to the cascade through the 6.0 MeV state. The GEANT simulation of the $4^+$ case and of the $\alpha$-source study predicts a transmission 13% higher than the measurements. We have adjusted the entire set of GEANT predictions by this factor and have assigned an uncertainty of 25% for recoil acceptance (except where this would imply a transmission >100%).

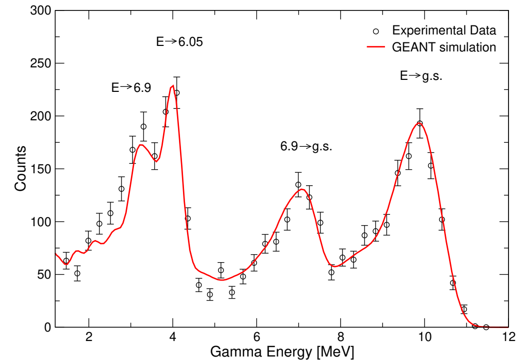


FIG. 1: Added BGO spectra at 0.898 MeV/u (data points) and GEANT simulation (line) of this run. The E→6.0 MeV transition is visible at about 4 MeV.

The $\gamma$-ray detection efficiencies of the individual detectors in the DRAGON BGO array have been previously simulated in GEANT as well as measured with several $\gamma$-ray sources in different geometries [9]. For the present experiment, the simulations were extended for the multiple $\gamma$-ray transitions in $^{12}$C$(\alpha,\gamma)^{16}$O. Since for the E→6.0 MeV transition we are typically dealing with a primary 3-6 MeV $\gamma$-ray, we are in an energy region which overlaps very well with previous simulations and calibrations. We therefore estimate the error in the $\gamma$-ray efficiency to be about 5%. In particular, in GEANT the cascade decay through the 6.0 MeV state was simulated including the $e^+e^-$ decay of this state to the ground state [10]. Largely a pure $E2$ decay pattern was assumed for the primary decay, except for the case of the $1^-$ E=5.23 MeV and the E=2.4 MeV $1^-$ resonances where we confirmed the transition to the 6.0 MeV state. Unfortunately the number of off-resonance counts in most spectra is too low to derive experimental angular distributions for this transition. The $R$-matrix fits presented below indicate that the $E1$ part of the cross section is more prominent than initially assumed. However, as the possible error resulting from different angular distributions is found to be small and taken into account, we did not try to adapt in a circular way the data reduction to the $R$-matrix fits. Fig. 1 shows a BGO spectrum taken at 0.898 MeV/u and a GEANT simulation. The yield for the E→6.0 MeV transition was then determined from these fits.

The total $^{12}$C current was monitored at the beginning of each run at a Faraday cup close to the entry into the gas target and continuously after the first electric dipole at another Faraday cup in the deflected beam position. We chose the $5^+$ at lower energies or the $6^+$ charge state of $^{16}$O or $^{12}$C at higher energies to be transported through DRAGON. In a previous work [11], we determined charge-exchange cross sections and under what conditions an equilibrium charge state distribution

TABLE I: Error budget for the E→6.0 MeV transition.

| error cause | value |
|---|---|
| DRAGON acceptance/mistuning[a] | +18%, -25% |
| angular distributions | 5% |
| number of target atoms | 10% |
| branching ratio | 10% |
| charge state fraction $^{12}$C | 5% |
| charge state fraction $^{16}$O | 5% |
| beam current integration | 3% |
| BGO array efficiency | 5% |
| DSSSD efficiency | 1% |
| Total error in S-factor | +31%, -25% |

[a]The error of the DRAGON acceptance.

is reached. Unfortunately that study did not cover the energy range used in this measurement, so we extended our studies with $^{12}$C and $^{16}$O beams. This measurement is reported in Ref. [6] and the results are used here. We attribute an error of 5% to charge-state uncertainties. At two resonances including the aforementioned $4^+$ resonance, we have measured $^{16}$O recoil yields in the $5^+$, $6^+$, and $7^+$ charge states and have refined our predictions in regard to recoil nuclei [12] showing that these only modify the result in negligible amounts within our errors.

Combining normalizations, branching ratios, acceptances and yields for the E→6.0 MeV transition leads to its excitation function after analyzing the $^{16}$O recoil spectra. We find that the separation of the $^{16}$O recoils in the focal plane of DRAGON is excellent. Therefore a single cut on the time-of-flight spectrum between the BGO and the DSSSD clearly selects coincidence $\gamma$ events without any random background taking all recoil events in the DSSSD into account.

While the BGO resolution is not sufficient to separate primary transitions to either the 6.0 or 6.1 MeV state in $^{16}$O, the necessary presence of a secondary 6.1 MeV $\gamma$ decay for the latter transition permitted us to clearly distinguish these two cases. For example, in the upper $4^+$ resonance, a clear secondary 6.1 MeV line can be identified. Such a line is largely absent in the spectra at other energies confirming that the transition seen indeed results from the first excited state of $^{16}$O, see Fig. 1. Two analyses have been made, either including or not including such a transition. For low statistics runs we find that the inclusion of a 6.1 MeV line often improves the fit. However, the sporadic appearance of such low statistics lines is not consistent with our knowledge of the $^{16}$O state structure and is also typically too weak to influence our results in a major way.

The excitation function shows both $2^+$ and $1^-$ resonances and is shown in combination with an $R$-matrix fit in Fig. 2. Systematic errors in the S-factor are listed in Table I. In a recent paper, Schürmann *et al.* [13] present a total $^{12}C(\alpha,\gamma)^{16}O$ reaction cross section measured at the recoil separator ERNA in approximately the same energy region as is covered here. As the E→6.0 partial

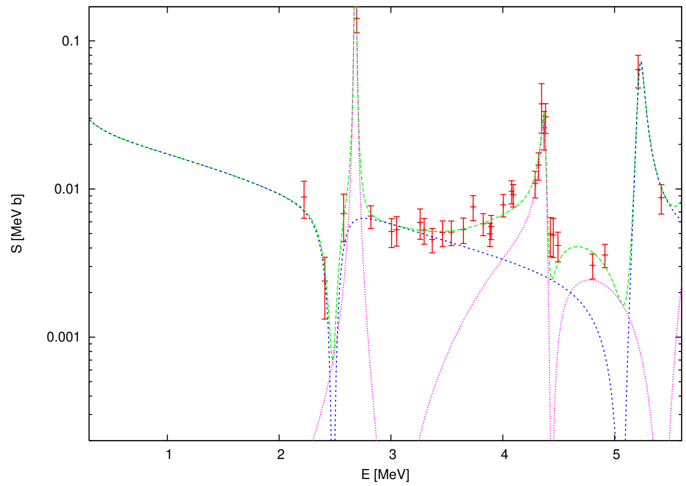


FIG. 2: Excitation function for the E→6.0 MeV transition in terms of center-of mass energies and S-factor including an $R$-matrix fit (positive $\theta_{f2}$, see text). The short-dashed line indicates the $E1$ transition, the dotted line the $E2$ transition, and the long-dashed line the sum of both.

cross section has to be a fraction of the total cross section of $^{12}C(\alpha,\gamma)^{16}O$, our data are indeed found below the S-factor values presented in Ref. [13], representing a considerable fraction of this cross section between resonances.

The $R$-matrix fits follow the procedure described by Barker and Kajino [4] including a direct or hard-sphere radiative component and an energy-dependent $\gamma$ width for the $E2$ capture. Boundaries were set on the $1^-$ and $2^+$ subthreshold states in $^{16}$O at E=-45 keV ($B_1$=-4.27) and E=-245 keV ($B_2$=-3.67), respectively. Apparent states in the fits were included as well as background states. The energies and $\alpha$-widths of these states were generally fixed to values derived from elastic scattering [14] due to the relatively low statistics of the present measurement, while the $\gamma$-widths and the $E2$ direct capture strength were allowed to vary freely. The $1^-$ subthreshold state was ignored in $\gamma$-strength as its branching ratio to the 6.0 MeV state is reported to be immeasurably small [15], while the $2^+$ subthreshold state is included with the width and branching ratio from literature, but is found ultimately to be irrelevant. An interaction radius $a$ of 5.5 fm was chosen in accordance with Ref. [14]. As the data derived here are of too poor quality to sensibly restrict the interaction radius $a$, no variations of this radius were performed. We are, however, convinced that a reasonable range for the radius $a$, e.g. the one of Ref. [14], will lead to values of $S_{6.0}(300)$ well within the range of $S_{6.0}(300)$ which we derive by varying some parameters of the fit and from other sources of uncertainty. No target thickness effects have been included in the fit. The fit is based on single-channel theory. We use the program MINUIT [16] for finding parameters of minimum $\chi^2$.

We find two fits of nearly identical quality, but with different S-factors at 300 keV. One of the fits (positive

$\theta_{f2}$, see below) is shown in Fig. 2. The two fits can be distinguished by the sign of the reduced width amplitude $\theta_{f2}$ of the $E2$ direct capture which is either positive or negative. For the positive solution, we find a total $\chi^2$=23.6 and with 32 data points and 9 parameters, $\chi^2_\nu$=1.03. For the negative $\theta_{f2}$ solution, we find $\chi^2$=24.0 and thus $\chi^2_\nu$=1.04. The two fits lead to different S-factors at 300 keV: $S^+_{6.0}$(300)=29.4 keV b for the positive solution and $S^-_{6.0}$(300)=20.0 keV b for the negative solution. Structurally, both fits are similar due to the fact that a strong background in the $E1$ amplitude dominates the low-energy cross section for both fits. Any attempts to supress such an amplitude leads to non acceptable fits. The 'dip' in the E1 amplitude at the E=2.4 MeV position is due to the combination of a small $\gamma$ width and a large $\alpha$ width as well as the interference signs chosen. For the $E2$ amplitude, a complicated interference pattern between the background state, the 13 MeV state and the direct capture is necessary to reproduce the excitation function. However, in the low-energy region, the $E2$ component can not produce the observed energy dependence. Note, that the inclusion or removal of our two lowest energy points only marginally influences the result.

To estimate the range of $S_{6.0}$(300), we have varied several parameters. In particular, we find that the dependence upon the $\gamma$-background strength $\gamma_{\gamma 41}$[19] is strong and that $S_{6.0}$(300) is well correlated with this parameter. We find a range of likely values $S_{6.0}$(300) by allowing a reasonable $\chi^2$ increase of 9 (corresponding to a statistical $3\sigma$ error) to be our error range, as we are not entirely sure if other ranges of S-factors may be found in other kinds of scans. We find for the positive $\theta_f$ solution $S^+_{6.0}$(300)=29±8 and for the negative $\theta_f$ solution $S^-_{6.0}$(300)=20±9. We have varied our data globally by the -25%, +31% constant systematic error found in Table I. Added in quadrature with the previous statistical errors we find for the positive $\theta_{f2}$ solution $S^+_{6.0}(300)=29^{+12}_{-11}$ and for the negative $\theta_{f2}$ solution $S^-_{6.0}(300)=20^{+11}_{-10}$. Because we feel that improved data will certainly lead to a unique solution for the extrapolation to 300 keV, we average both results and take the extremes of the errors as ultimate limits to give

$$S_{6.0}(300) = 25^{+16}_{-15}\ \mathsf{keV\,b}\ . \tag{1}$$

The cross section of the radiative capture of $\alpha$ particles into the first excited state of $^{16}$O has been neglected in previous discussion and literature. However, for any precision determination of the stellar $^{12}C(\alpha,\gamma)^{16}O$ reaction rate, it is now demonstrated to be required. If one assumes a total S-factor S(300)=170 keV b for static helium burning, as argued from elemental nucleosynthesis [1], the S-factor derived here represents about 15% of the total, certainly not negligible, if a precision of $^{12}C(\alpha,\gamma)^{16}O$ of 10% or better is demanded. Indeed, we find it likely to be the strongest cascade transition. The data and fits indicate a very complex relation between $E1$ and $E2$ capture with large $\gamma$-background terms in both components. Certainly better data with a separation of the $E1$ and $E2$ component, i.e. measurements of angular distributions, are most desirable as well as an extension of the energy range of the data.

We would like to acknowledge the help of the ISAC operators. In particular, we wish to thank R. Laxdal and M. Pasini in tuning the ISAC accelerator. We also wish to thank C. Galt and K. Oraas for working on GEANT simulations as well as the help of S. Engel during the data taking. This work was supported in part by the U.S. Department of Energy, under Grant No. DE-FG02-88ER40387. The financial contribution of NSERC to the DRAGON collaboration and of the government of Canada to TRIUMF is also acknowledged.

---


[1] T.A. Weaver and S.E. Woosley, Phys. Reports, **227**, 65-93 (1993).

[2] L.Buchmann and C.A. Barnes, Nucl. Phys. A, **777c** 254 (2005).

[3] L. Buchmann, Phys. Rev. C., **64** 022801(R) (2001).

[4] F.C. Barker and T. Kajino, Aust. J. Phys., **44** 396 (1991).

[5] D.A. Hutcheon *et al.*, Nucl. Inst. Meth. A, 498 190 (2003).

[6] W.R. Hannes, Praktikumsreport, unpublished, TRIUMF (2005).

[7] S. Engel *et al.*, Nucl. Inst. Meth. A, 553 491 (2005).

[8] http://wwwasd.web.cern.ch/wwwasd/geant/

[9] D. Gigliotti, Master thesis, UNBC (2004).

[10] S. Gorodetzky *et al.*, Phys. Rev. **131** 1219 (1963).

[11] W. Liu *et al.*, Nucl. Inst. Meth. A, 496 198 (2003).

[12] J. Zylberberg *et al.*, Nucl. Inst. Meth. B, in print, (2006).

[13] D. Schürmann *et al.*, Eur.Phys.J. **26** 301 (2005)

[14] P. Tischhauser *et al.*, Phys. Rev. Lett., 88 072501 (2002).

[15] D.R. Tilley et al., *Nucl. Phys. A*, **564** 1 (1993).

[16] "MINUIT, Function Minimization and Error Analysis"", CERN Program Library Entry D506 (unpublished).

[17] To simplify the reading, we quote energies of states in $^{16}$O only to the second significant digit and omit the leading '$E_x$='. Similarly, we often omit '$J^\pi$=' when quoting spin and parity of states in $^{16}$O.

[18] The maximum recoil angle varies from 20 to 18 mrad for the energy range covered. Cascade transitions, however, also populate smaller recoil angles.

[19] $\gamma$-width amplitude of the $4^{th}$ state in the fit to $\ell$=1.